Electronic Supplementary Information

Dissociative reaction of $[Au_{25}(SR)_{18}]^-$ at copper oxide nanoparticles and formation of aggregated nanostructures

Jayoti Roy, [a] Biswajit Mondal,[a] Gaurav Vishwakarma,[a] Nonappa,[b] Nishanthi Vasanthi Sridharan,[a] Pattabiraman Krishnamurthi,[a] Thalappil Pradeep*[a,c]

[a]DST Unit of Nanoscience (DST UNS) & Thematic Unit of Excellence (TUE), Department of Chemistry, Indian Institute of Technology Madras, Chennai 600036, India.

[b]Faculty of Engineering and Natural Sciences, Tampere University, FI-33720 Tampere, Finland.

[c]International Centre for Clean Water, 2nd Floor, B-Block, IIT Madras Research Park, Kanagam Road, Taramani, Chennai 600113, India.

Table of contents

Calculation of number of particles/ml for:

a) $[Au_{25}(PET)_{18}]^-$ cluster

Molecular weight = 7391

Mass of 1 $[Au_{25}]$ NC (m) = $\frac{7391^x 10^3}{6.023\times10^{23}}$ mg = $1.227*10^{-17}$ mg

Mass of $[Au_{25}]$ NC in 1 ml of stock solution considered in the experiments (W) = $\frac{1mg}{100ml}$

No of $[Au_{25}]$ NC in 1 ml of stock solution/1ml = (W/m)

$= \left(\frac{0.01}{1.227*10^{-17}}\right)$ No/ml

$= (8.15 * 10^{15})$ No/ml

Molarity of NCs in the stock solution = $(\frac{N}{N_A})$

$= \frac{8.15*10^{15}}{6.023*10^{23}}$ M

= 1.35 nM

Amount of stock solution was used during reaction – 25 µL.

b) CuO nanoparticles

Average size of CuO NPs (HRTEM) = 2R = 50 nm

Volume of 1 CuO NP (sphere), V = $\left(\frac{4}{3}\right)\pi R^3$ nm^3

= 65416.6 nm^3

Density of CuO NP, ρ = 6.31 g/ cm^3

= $(0.631*10^{-17})$ mg/nm^3

Mass of 1 CuO NP, m = V*ρ

=$(65416.6 * 0.631*10^{-17})$ mg

= $4.13*10^{-13}$ mg

Weight of CuO NPs (dry weight of the sample), W = 1.6 mg/ml

No of NPs in the solution, N = $(\frac{W}{m})$

= $4.019*10^{12}$ number/ml

Molarity of the CuO NPs in solution = $(\frac{N}{N_A})$

= $6.67*10^{-3}$ nM

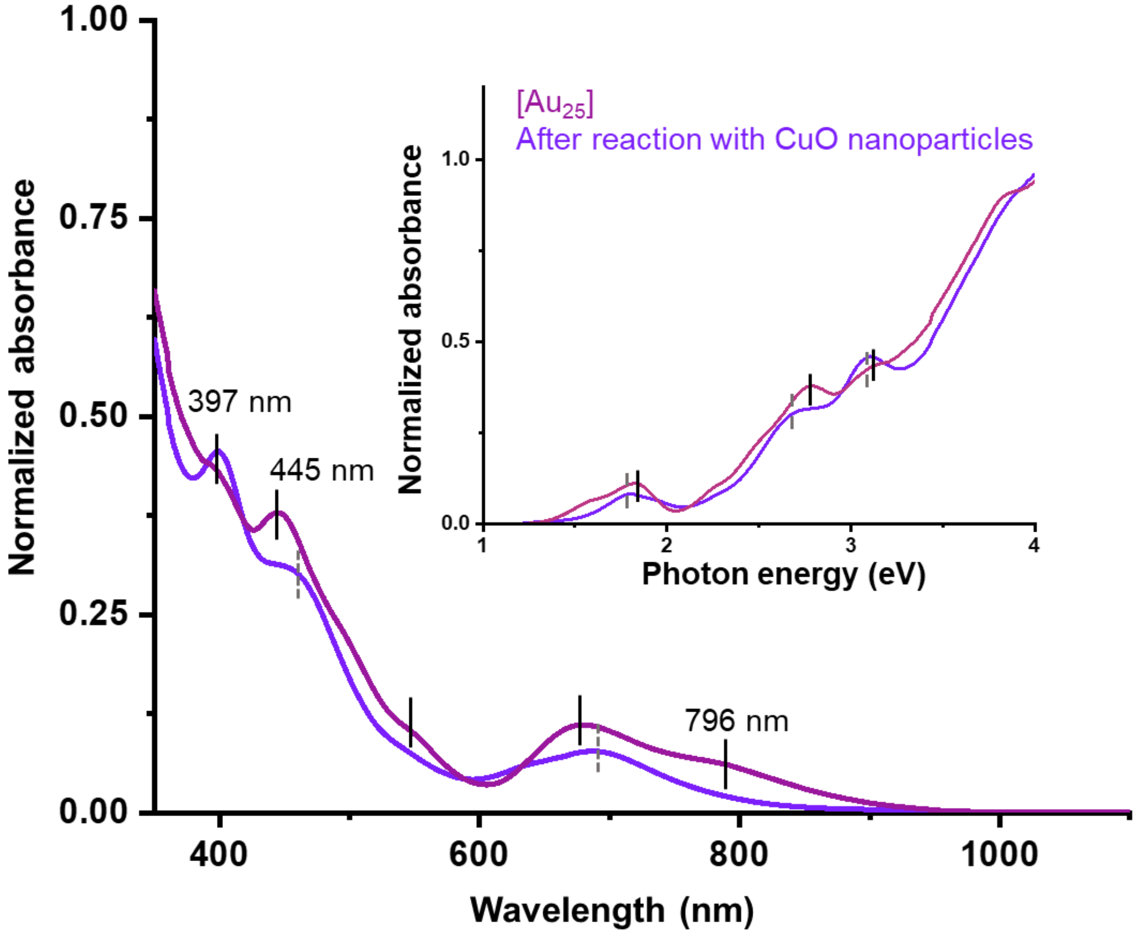

Fig. S1 UV-vis spectra of [Au_{25}] before and after the reaction. Inset shows the absorption spectra in terms of photon energy (eV) of [Au_{25}] before and after of the reaction.

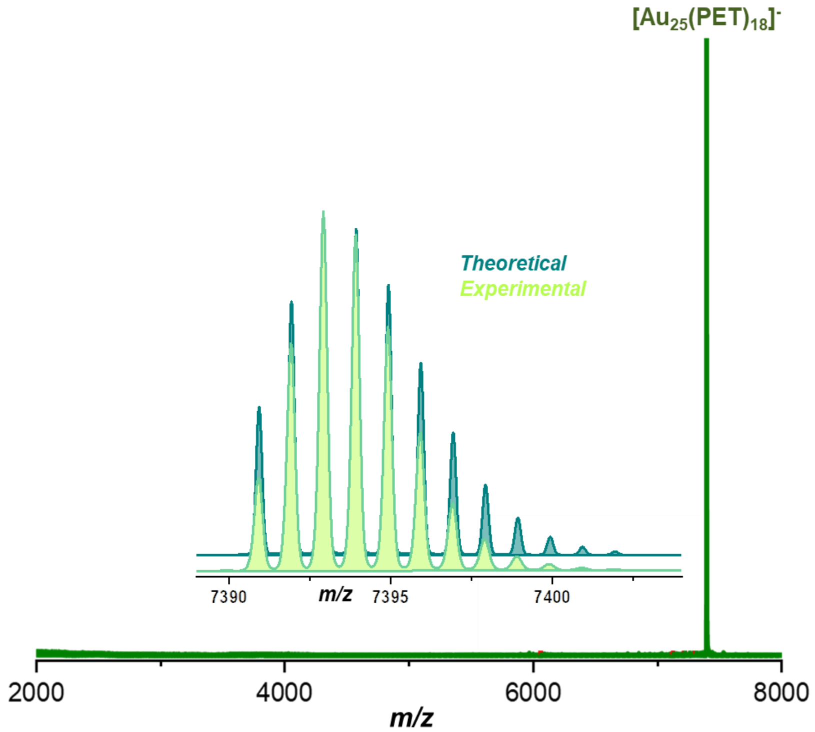

Fig. S2 ESI MS of $[Au_{25}]$ in DCM in the negative mode. The overlay plot of the experimental (light green) and calculated (dark green) isotopic distributions of $[Au_{25}]$.

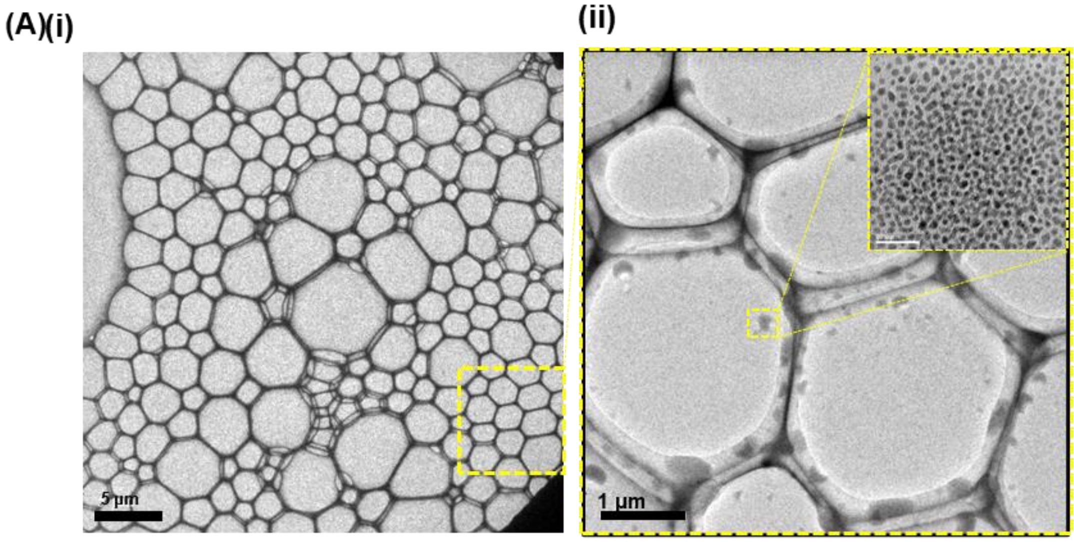

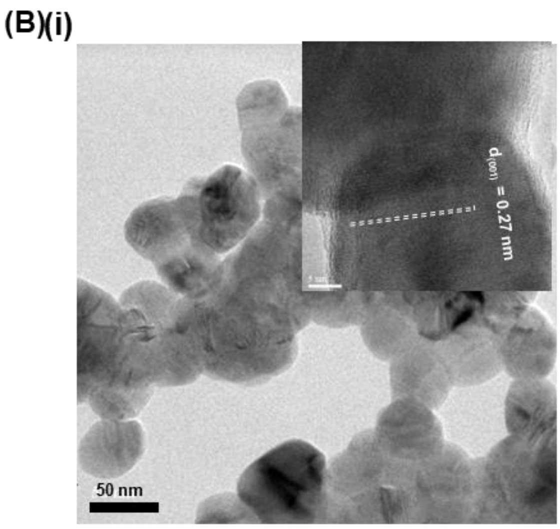

(ii)

Element	Atomic%
O	53.82
Cu	46.18
Total	100

Fig. S3 (A(i-ii)) TEM micrographs of drop casted [Au_{25}] NC. In inset of (A(ii)) shows the discrete NCs (slight beam-induced aggregation and damage are also observed). (B(i)) TEM image of bare parent CuO NPs. Inset shows the lattice spacing of crystalline NPs. (B(ii)) EDS elemental compositions of parent NPs.

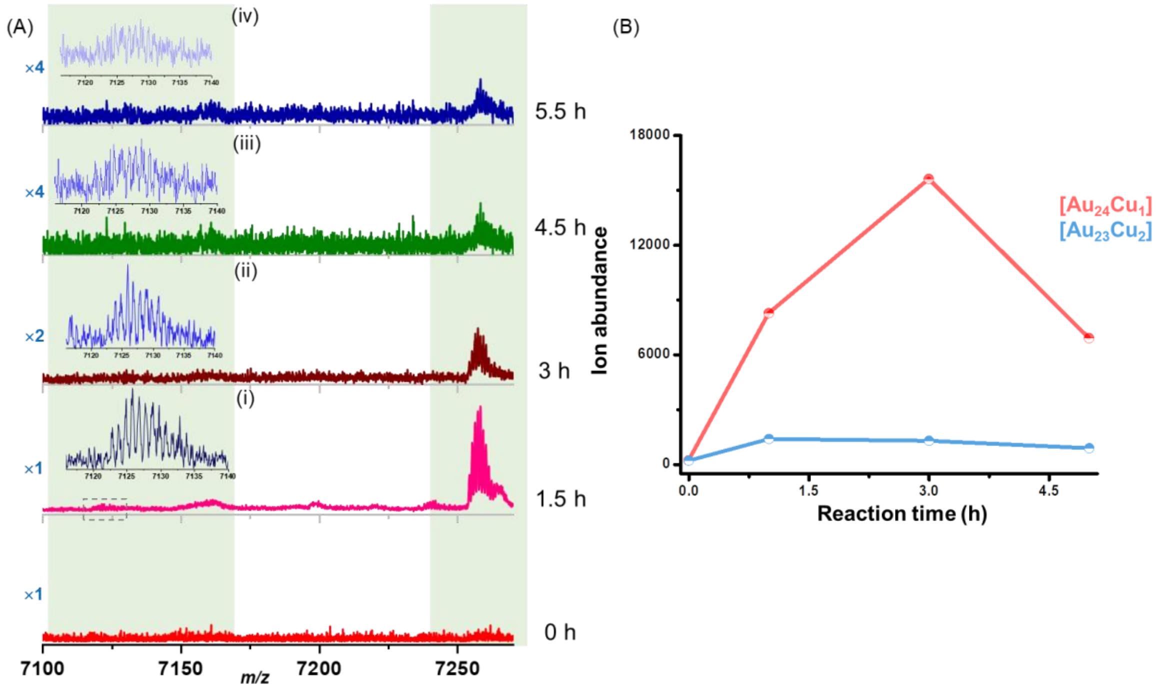

Fig. S4 ESI MS spectra (A) of the evolution of [$Au_{24}Cu_1$] and [$Au_{23}Cu_2$] NCs during the reaction and their ion abundance plot (B) as a function of reaction time.

(A)

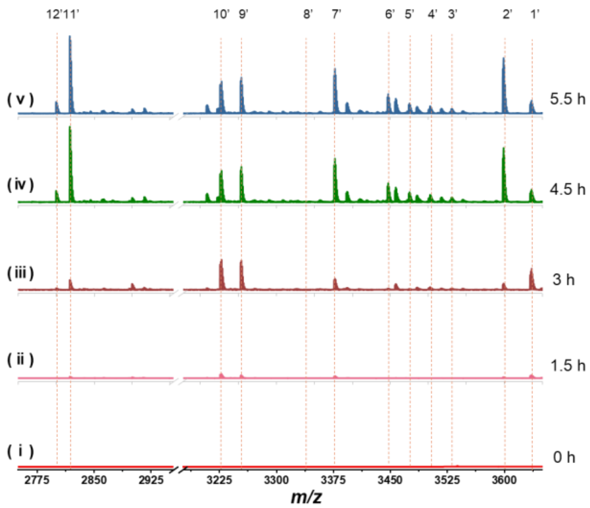

(B)

Sl no.	Molecular formulae	Sl no.	Molecular formulae
1’	$[Au_{11}(PET)_{10}CuO_2]^-$	7’	$[Au_{10}(PET)_{10})]^-$
2’	$[Au_{11}(PET)_{10}(O_2)_2]^-$	8’	$[Au_{10}(PET)_{10}O_2]^-$
3’	$[Au_9(PET)_{12}O]^-$	9’	$[Au_{10}(PET)_9O_2OH]^-$
4’	$[Au_8Cu(PET)_{10}(TOA)O]^-$	10’	$[Au_9(PET)_{10}CuOH]^-$
5’	$[Au_7(PET)_{12}(TOA)O]^-$	11’	$[Au_8(PET)_9O]^-$
6’	$[Au_9Cu_2(PET)_{11}]^-$	12’	$[Au_8(PET)_9]^-$

Fig. S5 ESI MS of smaller NCs fragments generated with time and (B) table of chemical compositions of the fragments.

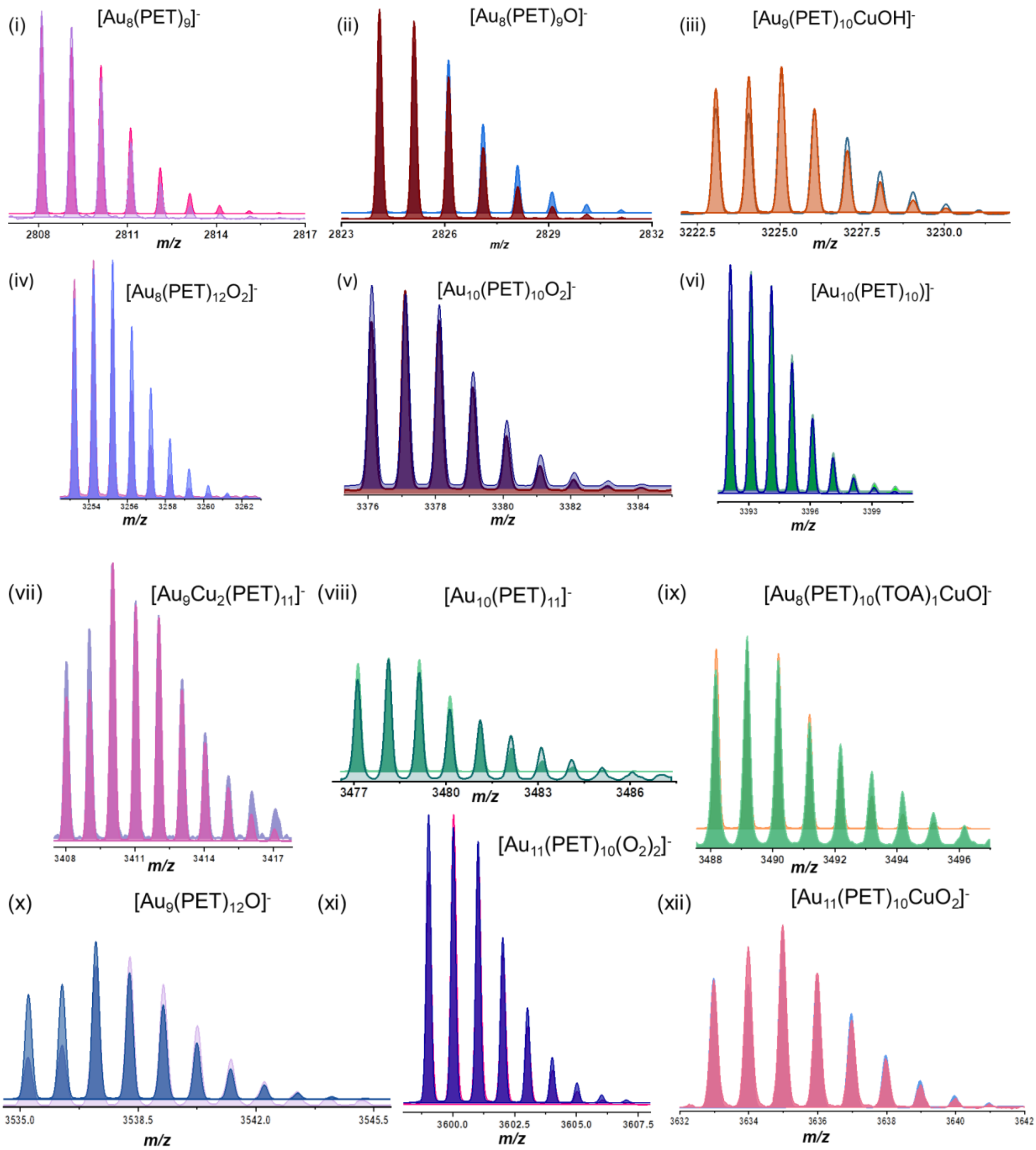

Fig. S6 Experimental high-resolution isotopic distribution of smaller NC fragments with their calculated isotopic distributions.

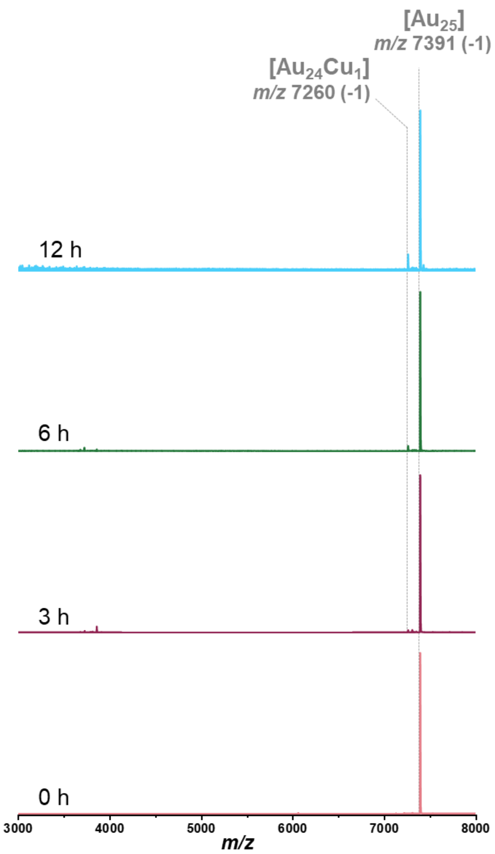

Fig. S7 Time-dependent ESI MS of reaction between [Au_{25}] and very diluted CuO NPs solutions.

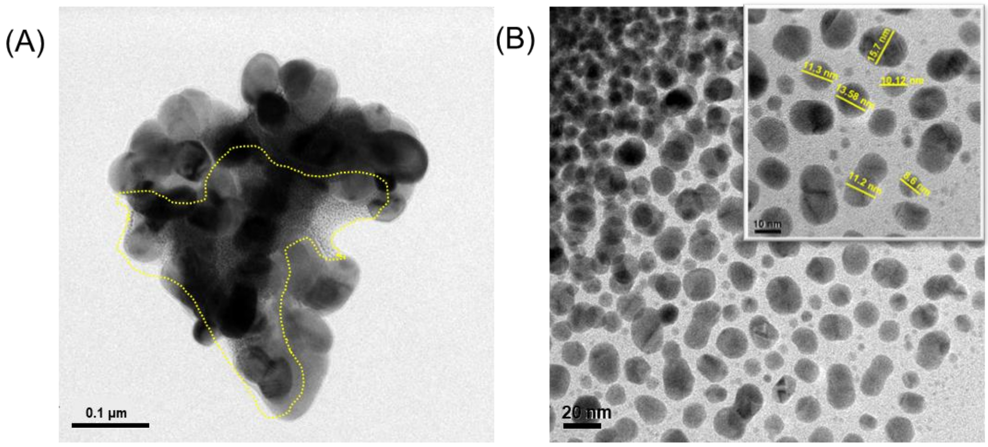

Fig. S8 TEM micrographs show bare CuO NPs after the reaction. In (A) and (B), the bare NPs are intermingled with NC (area under dotted line), and smaller size bare NPs are shown, respectively.

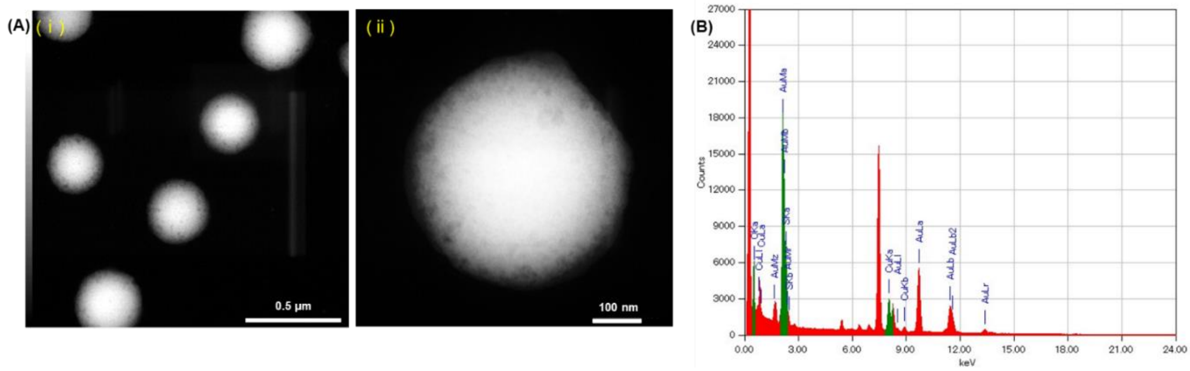

Fig. S9 (A(i-ii)) STEM micrographs of nano-assemblies and (B) EDS spectrum collected from (A(ii)) Showing the elemental compositions.

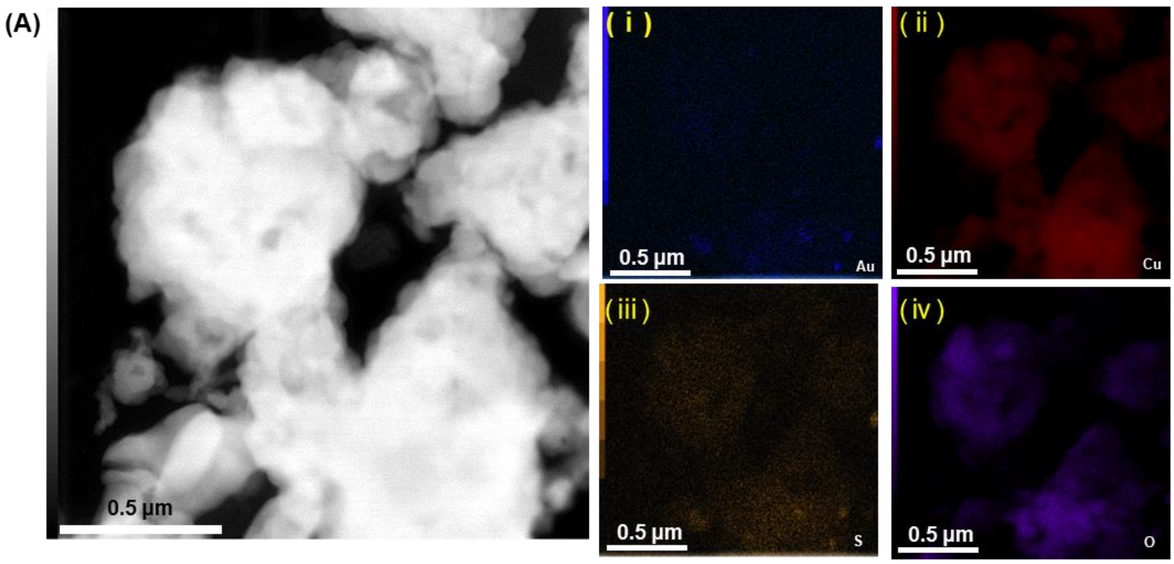

Fig. S10 (A) STEM image and EDS elemental mapping of NPs after the reaction.

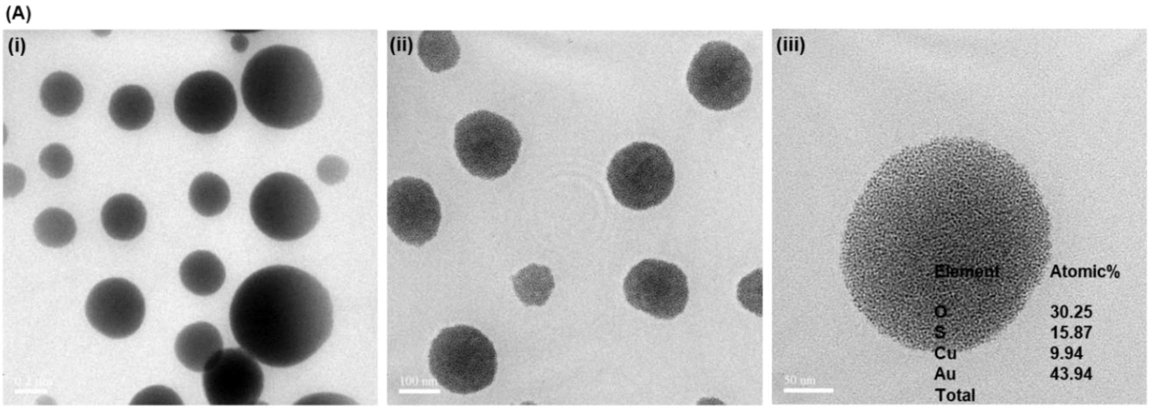

Fig. S11 TEM micrographs of NCs present in the supernatant and respective elemental compositions (in inset).

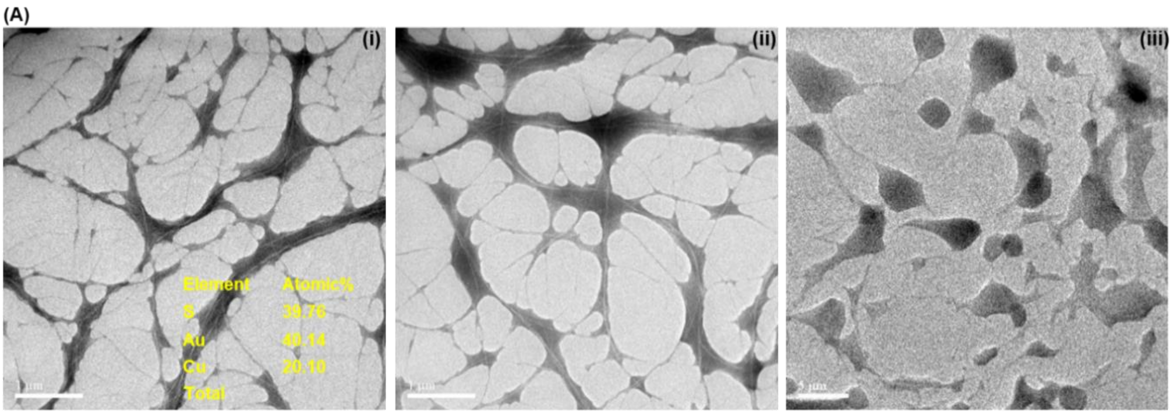

Fig. S12 TEM photographs of NCs present in the supernatant and respective elemental composition (in inset of (i)).

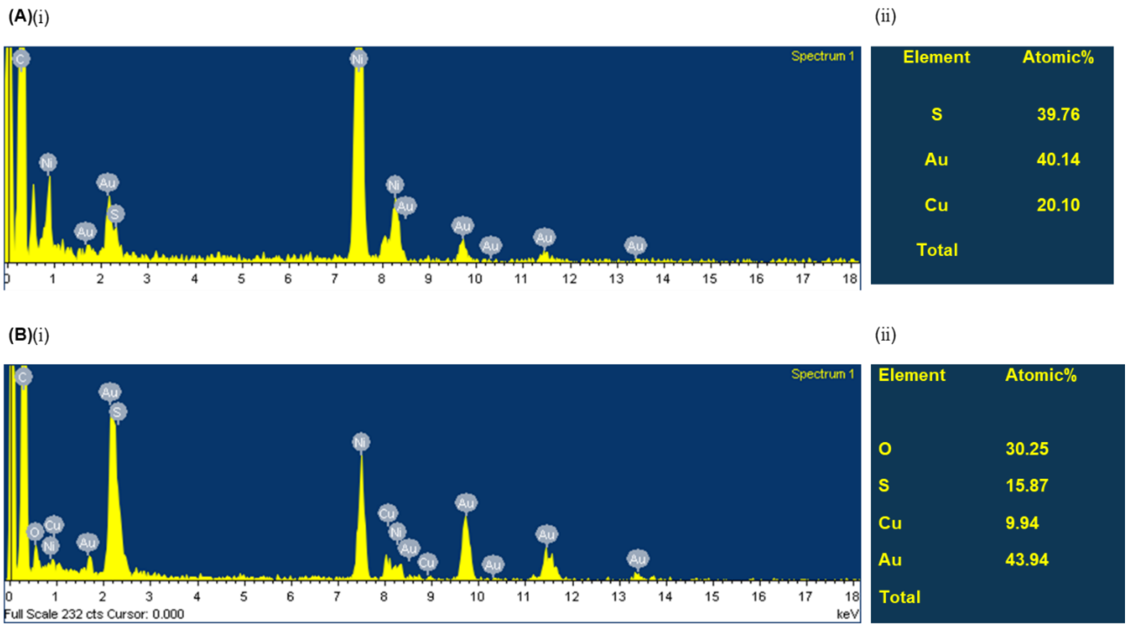

Fig. S13 Elemental compositions from EDS spectrum of – (A(i-ii)) supernatant containing NCs, and (B(i-ii)) isolated NSs. The Ni signal is coming from the grid (carbon coated Ni grid is used for the imaging).

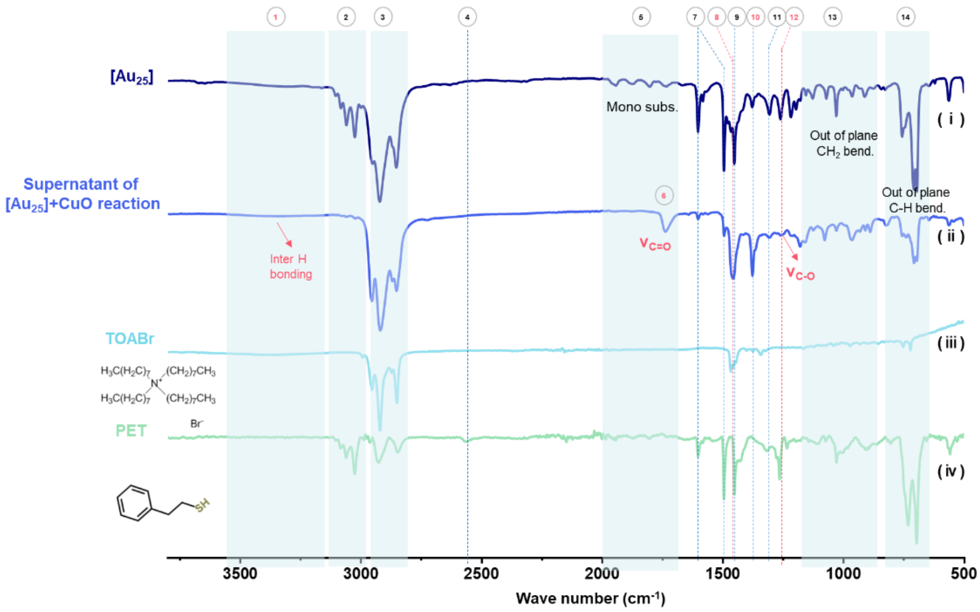

Sl. no	IR peak
1	Intra H bonding
2	Aro. C-H stret.
3	Aliph. C-H stret.
4	Free S-H
5	Aromatic-out of plane C-H bending, progression band
6	C=O stret.
7	C=C stret.
9	C-O stret.
8,10	S=O stret.
11	C=C bend. alk.
12	C-O alko.
13	Out of plane CH_2 bend.
14	Out of plane SP^2 C-H bend

Fig. S14 FTIR analysis of (i) [Au_{25}] NC, (ii) supernatant of the reaction, (iii) TOABr and (iv) PET (frequencies marked with red indicate new peaks appeared due to the reaction).

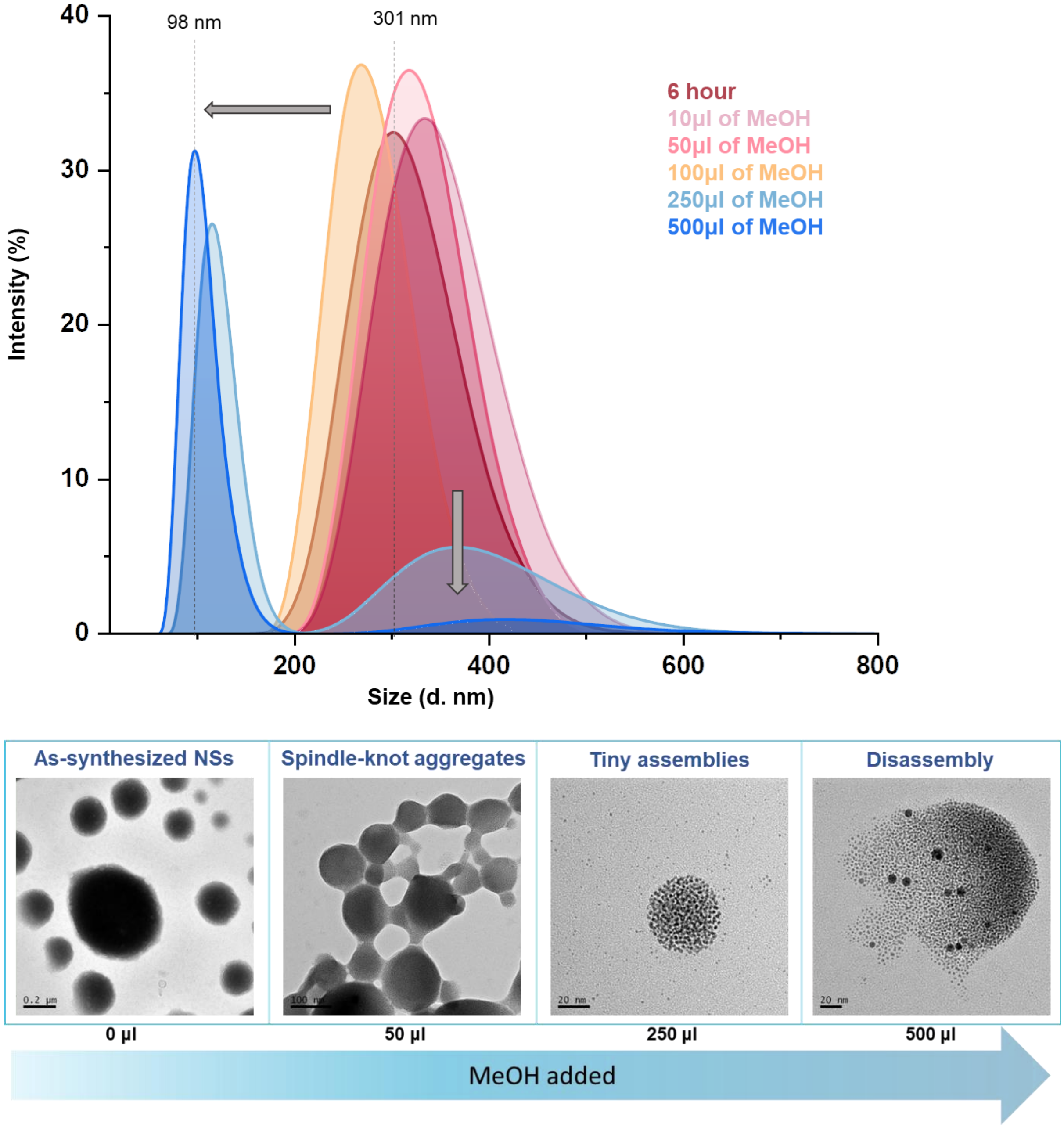

Fig. S15 DLS study and TEM images showing gradual disassembly, from NSs to smaller aggregates.

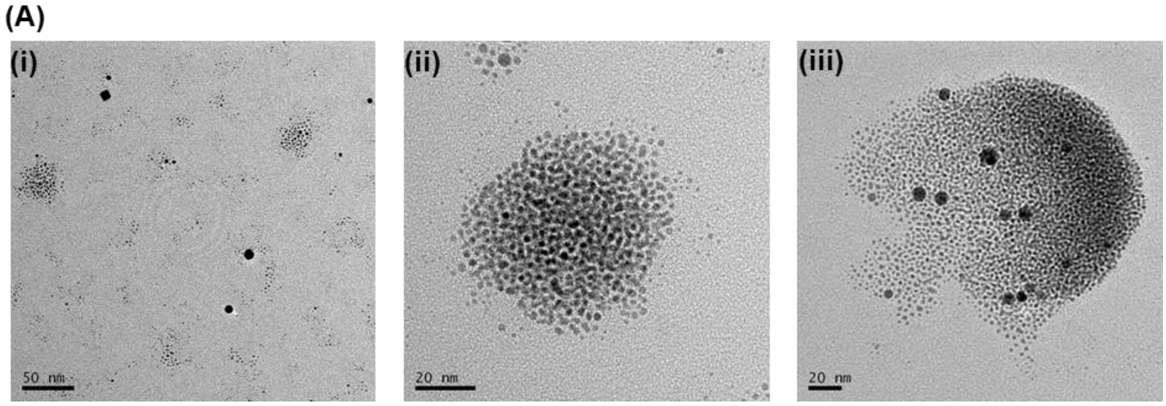

Fig. S16 TEM images of disassembled NSs after addition of 500 μl of MeOH.